Published in final edited form as:
IEEE Trans Neural Syst Rehabil Eng. 2014 July ; 22(4): 886–898. doi:10.1109/TNSRE.2014.2298362.

Development of a Biomimetic Hand Exotendon Device (BiomHED) for Restoration of Functional Hand Movements Post-Stroke

Sang Wook Lee[1,2], **Katlin A. Landers**[1,2], and **Hyung-Soon Park**[3,4,*]

[1]Department of Biomedical Engineering, Catholic University of America, Washington, DC, USA

[2]Center for Applied Biomechanics and Rehabilitation Research, Medstar National Rehabilitation Hospital, Washington, DC, USA

[3]Mechanical Engineering Department, Korea Advanced Institute of Science and Technology, Daejeon, Republic of Korea

[4]Rehabilitation Medicine Department, National Institute of Health, Bethesda, MD, USA

Abstract

Significant functional impairment of the hand is common among stroke survivors and restoration of hand function should be prioritized during post-stroke rehabilitation. The goal of this study was to develop a novel biomimetic device to assist patients in producing complex hand movements with a limited number of actuators. The Biomimetic Hand Exoskeleton Device (BiomHED) is actuated by exotendons that mimic the geometry of the major tendons of the hand. Ten unimpaired subjects and four chronic stroke survivors participated in experiments that tested the efficacy of the system. The exotendons reproduced distinct spatial joint coordination patterns similar to their target muscle-tendon units for both subject groups. In stroke survivors, the exotendon-produced joint angular displacements were smaller, but not significantly different, than those of unimpaired subjects (p = 0.15–0.84). Even with limited use of the BiomHED, the kinematic workspace of the index finger increased by 63–1014% in stroke survivors. The device improved the kinematics of the tip-pinch task in stroke survivors and resulted in a significant reduction in the fingertip-thumb tip distance (17.9 ± 15.3 mm). This device is expected to enable effective ‘task-oriented’ training of the hand post-stroke.

Keywords

Hand; stroke; orthosis; biomimetic; exotendon; task-oriented training

I. Introduction

Significant upper extremity impairment is prevalent among stroke survivors [1,2] and recovery of upper extremity function is often slower and more limited than for the lower extremities [3]. Specifically, motor deficits of the distal hand components are known to be

*Corresponding author Address: 291 Daehak-ro, Yuseong-gu, Daejeon 305-701, Republic of Korea hyungspark@kaist.ac.kr.

more significant than those of the proximal arm [4,5]. Restoration of lost hand function should be prioritized in stroke rehabilitation due to its importance in upper extremity functional activities [6,7].

High intensity, task-oriented training has been shown to maximize outcomes in stroke rehabilitation [8,9]. Therefore, repetitive practice of functional hand tasks should be incorporated into rehabilitation programs to effectively restore hand function. The complex nature of manual tasks, however, poses a significant challenge to the implementation of task-oriented training for hand rehabilitation. Most manual tasks require complex spatiotemporal coordination of multiple joints (i.e., kinematics) [10] and/or multiple degrees-of-freedom (DOF) force control (i.e., kinetics) [11,12], which makes repetitive practice of functional hand movements very challenging. Many stroke survivors have uncontrolled spasticity or weakness [13], which typically results in a clenched-hand posture [14] and limits their ability to perform manual tasks without assistance. Even after stroke survivors regain the ability to open their hands, functionality may remain limited due to a variety of impairments affecting task performance. For example, diminished capacity to voluntarily modulate muscle activities [15,16] or abnormal interactions between hand flexors and proximal muscles [17] can result in abnormal hand kinematics and kinetics, which may further lead to reduced workspaces [18], abnormal joint coordination [19], and misguided force at the thumb tip [15] and fingertip(s) [20]. Even if rigorous training could be performed with the help of skilled therapists, it would be labor-intensive and expensive, imposing a significant economic burden on patients.

Recently, a number of robotic devices have been developed for hand rehabilitation. These devices offer the ability to cost-effectively administer training of repetitive hand movements, but inherent functional limitations often limit their efficacy. Many robotic devices are designed to explicitly assist with hand opening [21], as significant impairment in finger extension typically emerges after stroke [14]. Other devices provide assistance with both finger extension and flexion [22] and enable simple functional tasks (e.g., grasping) [23,24] through execution of pre-determined patterns of coupled movements within-and between-digits. The complexity and functionality of these tasks, however, are limited in comparison to the rich repertoire of human manual tasks to be restored. Recent exoskeletons with more complex design [25] can independently control individual finger joints, but in order to attain complex actuation mechanisms their peripheral structures tend to be bulky, which prevents users from practicing concurrent hand and arm movements. As task-oriented training of the upper extremity typically involves both arm and hand movements, it is crucial to design a compact light-weight device for hand training that can be combined with existing arm devices [26,27].

An effective assistive device for hand rehabilitation should be capable of providing specific assistance patterns reflecting the dynamic function of impaired hand muscle-tendon units (i.e., reproducing spatial joint coordination patterns generated by the tendons), but most current devices cannot consider and incorporate such subject-specific impairments into training. Generally, in stroke rehabilitation, targeted assistance of an impaired muscle is achieved by isolating a specific joint movement for which the impaired muscle is the single major agonist and providing assistance with that motion [26,28]. Unlike most joints with one

or two agonists, finger joint coordination is achieved by spatiotemporal coordination of multiple muscles [29–31], and most hand muscles produce coordinated multi-joint torque patterns [32,33]. In stroke survivors, these complex dynamics are often impacted by unbalanced impairment in which certain sub-movements of muscle-tendon units are more severely impaired than others. Most existing systems are designed to reproduce movement kinematics (i.e., joint coordination) of the entire hand and these devices can neither provide targeted assistance to impaired muscles, nor can they reinforce (or counteract) deficient or abnormal sub-movements.

Therefore, the purpose of this study was to develop and test a novel hand exoskeleton device that addresses the aforementioned limitations of current devices by adopting a 'biomimetic' design approach, with which complex hand movements are generated with a limited number of actuators. This device allows performance of coordinated joint movements through actuation of 'exotendons' that replicate the dynamic function (i.e., spatial coordination of joint torques) of the major hand muscle-tendon units. The peripheral complexity of the proposed device plays a critical role in functional movement generation, similar to the behavior of the neuromechanical system of human hand [34]. As the exotendons 'mimic' the anatomy of the major hand muscle-tendon units, the joint coordination patterns produced by the exotendons should allow reconstruction of multiple functional hand movements.

This paper describes the mechanical design of the proposed system, as well as the results of three pilot experiments designed to evaluate system performance. First, the dynamic function of the exotendons was evaluated using a system identification approach, followed by testing the efficacy of restoration of the kinematic workspace of the finger in stroke survivors. Finally, the ability to restore the proper mechanics of functional task performance (i.e., the tip-pinch task) was evaluated. Specifically, since inappropriate compensatory strategies may impair recovery post-stroke [35,36], the device was used to prevent patients from adopting compensatory strategies that are often observed in stroke survivors during functional hand movements [37].

II. Methods

A. Device Design

1) Mechanical structure—The hand exoskeleton device used in this study, the Biomimetic Hand Exotendon Device (BiomHED), is a cable-driven exoskeleton-type device that is worn as a glove. A zipper sewn on the palmar side of the glove facilitates donning and doffing. The fingers are controlled by four cables that mimic the geometry of the four major finger muscle-tendon units: the extensor digitorum communis (EDC), the flexor digitorum profundus (FDP), and the radial and ulnar interossei (RI and UI). The thumb is controlled by four cables that replicate the anatomical structure of the four thumb muscle-tendon units: the extensor pollicis longus (EPL), the flexor pollicis longus (FPL), the abductor pollicis longus (AbPL), and the adductor pollicis longus (AdPL). Four devices with identical designs, two for the right hand and two for the left hand (one small and one large glove for each side), were prototyped and used in this study.

For each finger, four cables (SAVA 1024, Sava Industries Inc., Riverdale, NJ, USA) were routed through custom thermoplastic guides (thickness 4 mm) attached to the dorsal and palmar aspects of the glove (Fig. 1) such that tension applied to each of these cables produced coordinated finger movements. Each thermoplastic piece was shaped after applying heat to the material and holes (diameter 1 mm) were routed through the plastic to ensure that each cable maintained the intended orientation.

The first Finger ExoTendon (FET_1) replicates the anatomical configuration of the EDC, a major finger extensor muscle-tendon unit that produces concurrent extension of all three joints: the distal interphalangeal (DIP), proximal interphalangeal (PIP), and metacarpophalangeal (MCP) joints [33,38]. FET_1 runs through the center hole of each of the three guides attached to the dorsal aspect of each digit (dorsal guides; Fig. 1a) and delivers concurrent extension moments to the three joints of the finger. The second finger exotendon (FET_2) replicates the anatomy of the FDP, a major finger flexor muscle-tendon unit that produces concurrent flexion of all three joints [39,40]. This cable runs through two thermoplastic guides attached on the palmar aspect of the distal and proximal phalanges (palmar guides; Fig. 1c) and provides concurrent flexion moments to all three joints. The geometry of the third and fourth exotendons (FET_3 and FET_4) resembles the anatomical pathways of the radial and ulnar interosseous muscle-tendon units of the finger (RI and UI). These two cables originate from the guide attached to the dorsal aspect of the distal phalanx and are routed such that these exotendons pass near the center of the PIP joint. The guide attached on the proximal phalanx directs these exotendons to the palmar aspect of the MCP joint (Fig. 1a and b). Thus, FET_3 and FET_4 produce small extension moments at the DIP and PIP joints, but produce larger flexion moments at the MCP joint of the finger. FET_3 and FET_4 were connected in parallel at the wrist and are, therefore, controlled together (Fig. 2).

Four cables enabled movements of the thumb. Similar to FET_1 and FET_2 of the finger, the first and second Thumb ExoTendons (TET_1 and TET_2) replicated the anatomical structure of the EPL and FPL tendons and were routed along the dorsal and palmar aspects of the thumb, respectively. These two exotendons were designed to provide extension (TET_1) and flexion (TET_2) moments to all three joints of the thumb: the interphalangeal (IP), the first MCP (MCP_1), and the first carpometacarpal (CMC_1) joint. The third thumb exotendon (TET_3) was looped around the proximal phalanx of the thumb and routed along the dorsum of the hand in the ulnar direction, thus creating an adduction movement of the thumb. The fourth thumb exotendon (TET_4) was also looped around the proximal phalanx of the thumb, but in the radial direction, and crossed a pulley attached to the radial aspect of the first metacarpal bone. TET_4 thus produced an abduction moment about the CMC_1 joint. The four thumb exotendons (TET_1– TET_4) were designed to replicate the dynamic function of the major thumb muscle-tendon units [41].

The geometric moment arms of each exotendon with respect to the joint center were measured using an excursion method [39] in five subjects, during which the excursion of each exotendon and the corresponding angular displacement of the joints in the index finger and the thumb were measured. The magnitudes of the estimated geometric moment arms are summarized in Table 1.

2) Actuation—Actuators that transmit tension to the exotendons were placed on a forearm brace designed to be worn by subjects. Seven light-weight brushed DC motors with gearheads (A-max 16; GP 16A with reduction ratio 29:1; Maxon Motor AG, Switzerland) were attached to the brace via L-shaped brackets. A small L-shaped plastic channel that guided each exotendon to the corresponding motor was placed approximately 1 cm distal to each motor (Fig. 2). On the dorsal aspect of the forearm, the four FET_1s were conjoined near the wrist to form a single cable that was connected to the DC motor. Four linear tension springs were connected in parallel to the FET_1s to distribute the force equally among each of the four fingers (Fig. 2a). Similarly, on the ventral aspect, the four FET_2s were conjoined into a single cable and the eight $FET_{3/4}$s (4 FET_3s and 4 FET_4s) were conjoined into a single cable via four and eight tension springs, respectively. The cables were then connected to their respective motors (Fig. 2b). The four TETs (TET_1–TET_4) were individually connected to four motors.

This system was designed to be wearable, as the entire forearm apparatus including motors and the brace weighs less than 1 kg. Note that a design goal was to allow users to perform distal hand movements concurrently with proximal arm movements. This design allows practice of functional hand movements to be incorporated with various proximal arm movements and allows users to perform functional upper extremity movements such as ‘reach-and-grasp’ tasks.

B. Experiments

Three experimental protocols were implemented to test the performance of the prototype device. In the first session, the dynamic function of each exotendon (i.e., mapping of each exotendon force to multi-joint movements) was evaluated and the resulting coordination patterns were compared to those produced by the target muscle-tendon unit. In the second session, the capacity of the BiomHED to restore finger kinematics was examined. Specifically, the restoration of the functional workspace of the fingertip and multi-joint coordination patterns of the finger were evaluated. Finally, the device efficacy in reproduction of the kinematics of a representative functional manual task was tested.

The experimental protocol was approved by the MedStar Institutional Review Board and the Institutional Review Board of the Catholic University of America and written informed consent was obtained from each subject.

1) Subjects—Four subjects with chronic hemiparesis resulting from stroke and ten subjects with no history of neurologic disorders (4 females and 6 males; mean ± SD age = 25.4 ± 4.5 yr) participated in the study. Subject characteristics for the stroke survivors are summarized in Table 2.

2) Instrumentation—In all three sessions, joint angles of the fingers and the thumb were obtained during movements using an 8-camera motion capture system (Osprey Digital RealTime System; Motion Analysis Corp., Santa Rosa, CA, USA). Twenty-three small reflective markers (diameter 4 mm) were attached to the dorsum of the instrumented glove and the marker locations were recorded at 100 Hz for each trial. The temporal trajectory of each marker location was then digitally filtered forwards and backwards using a 3rd-order

Butterworth filter (MATLAB; MathWorks, Inc., Natick, MA, USA). Each joint angle was then computed from the spatial trajectories of the corresponding pair of markers.

3) Experimental Session 1 - Dynamic function of exotendons—In the first session, transformation of the force of each exotendon to angular displacements of the hand joints (i.e., the dynamic function of each exotendon) was examined by applying force to the individual exotendons and recording the resultant movements. The kinematic characteristics of the movement produced by each exotendon were compared to literature-reported values for the target muscle-tendon unit [33,39,40,42].

In this experiment, the device was worn by each subject (on the impaired hand for stroke survivors or on the dominant hand for control subjects). For stroke subjects, before the device is worn, their hands were stretched by the experimenters for three to four minutes, and the donning process typically took five to ten minutes. The exotendons were connected to the motor via bolt snap connectors after the glove was worn by the subjects.

All subjects were seated comfortably on a chair and instructed to rest their forearm on the table, with the table height adjusted according to each subject's seated height. Subjects were instructed to relax their hand so that they neither assisted nor resisted the movements produced by loading the exotendon. Before each experimental session, the digits were passively moved in order to check if the hand was relaxed. Additionally, before each exotendon force condition was applied, the hand was visually examined to verify if it returned to the neutral posture.

For loading of each exotendon, the force level was increased in three steps of equal magnitude (step length 2 sec) with the magnitude of each step set to 33.3% of the maximum force magnitude. The maximum force magnitude was initially set to 8 N for TETs and 10 N for FETs and was adjusted as needed over several trials for each subject. For example, the force magnitudes at all steps were decreased by 10% if any joint reached the full range of motion before the force reached the maximum value. Conversely, the force magnitudes were increased by 10% if the full range of motion was not achieved at the end of the trial (i.e., at the maximum force level). The current (or torque) control mode of the motor amplifier (ESCON 36/2, Maxon Motor AG, Switzerland) was used to operate the DC motors, which regulated the magnitude of current provided to the motor proportional to voltage input sent to the amplifier. The input voltage was sent using a custom-written Labview program (National Instruments Corp., Austin, TX, USA).

4) Experimental Session 2 - Kinematic finger workspace—In the second session, the kinematic workspace of the index fingertip accessed during voluntary movements was quantified and compared to the workspace accessed with the help of the BiomHED system. Two representative kinematic parameters, the location of the index fingertip and the within-digit joint coordination patterns, were computed from the marker locations recorded during these movements (see *C. Data Analysis*).

The kinematic workspace of the index fingertip accessed during voluntary finger movements was first estimated. Subjects were asked to place their hand on a plate on which fifteen

parallel lines were drawn (distance between any two neighboring lines 10 mm). The metacarpal bones (i.e., the palm) of the hand were placed such that the palm formed a right angle (90°) with each line. After placing the subject's hand on the plate, the orientation and the tilt angle of the table was adjusted to maintain the forearm in a neutral position with respect to supination/pronation. Stroke survivors were allowed to adjust their elbow flexion angle if they found it difficult to maintain a neutral forearm after table adjustment.

At each horizontal line oriented orthogonal to the subject's palm, the subjects first positioned their fingertip at the point closest to their hand and were then asked to move their fingertip along the line to the farthest point that they were able to reach on the line. Once they reached their maximum range of motion along a given line, the subjects repositioned their fingertip on the neighboring line and repeated the same procedure. Subjects were encouraged to start their movements from the most distal line (farthest from the wrist) to the most proximal line (closest to the wrist) (see Fig. 3). The same procedure was implemented for all subjects. However, stroke survivors were encouraged to take frequent rest breaks and to stretch their fingers between trials, if needed. Previous studies have used similar techniques to quantify finger workspace [18].

The kinematic workspace accessed during finger movements produced by BiomHED was then assessed. For this experiment, different exotendon-force combinations (i.e., loading conditions; LCs) were applied to demonstrate the capacity of BiomHED to explore the kinematic workspace of the finger. The three individual tendon LCs used in Session 1 (LC_1 = FET_1, LC_2 = FET_2, and LC_3 = FET_3) were tested. In addition, two other exotendon LCs, which involved concurrent loading of two exotendons, were tested to assess the finger movements enabled by the BiomHED system (LC_4 = the maximum FET_2 force identified in Session 1 and 30% of the maximum FET_1 force; LC_5 = the maximum FET_2 force and 50% of the maximum FET_3 force). Therefore, a total of 5 LCs (LC_1–LC_5) were used to sample the finger kinematic workspace accessed by the proposed system. Note that the five implemented exotendon LCs generate only a subset of the finger movement patterns that the device can produce. The purpose of this experiment was to demonstrate the performance of the device by producing a few distinct kinematic patterns of the finger, represented by the fingertip workspace and inter-joint coordination patterns (see *C. Data Analysis*).

5) Experimental Session 3 - Restoration of functional hand movements—To assess the capacity of the proposed device to enable functional hand movements, a tip-pinch task was selected as the target task, due to its importance in daily functional activities [43,44]. Both the kinematic and kinetic aspects of the pinch task are significantly impaired post-stroke [20,45,46]. In the tip-pinch task, subjects were instructed to perform the target task without assistance from the device (‘voluntary task performance’). Then, a combination of forces from the exotendons was applied with the aim of reproducing the kinematics of the target task (‘device-assisted task performance’).

The magnitude of the force applied to each exotendon during device-assisted task performance was determined from the force-joint angle relationships estimated during Session 1. Briefly, the spatial coordination patterns of the finger and thumb joints of unimpaired subjects were first examined during voluntary task performance. Given the

measured joint angles of these 'target' postures and the joint angle-exotendon force relationship of each subject estimated during Session 1 (i.e., p_{ij}^k and q_{ij} from Session 1; see *C. Data Analysis*), the coordination patterns of the exotendon forces were estimated for each subject.

C. Data Analysis

1) Session 1 - Dynamic function of exotendons—The transformation of the exotendon force to the angular displacement of the joint was experimentally identified from the measured joint angular displacements under individual exotendon loading conditions.

$$\theta_{ij}=g_{ij}^k(f_k) \quad (1)$$

θ_{ij}: joint angle of the i^{th} joint in the j^{th} digit

f_k: force applied to the k^{th} exotendon

$g_{ij}^k(\cdot)$: force-angle transformation function determining joint angle, θ_{ij}, produced by force f_k

i: joint/DOF of each digit (Thumb: 1 = IP_1 flexion, 2 = MCP_1 flexion, 3 = CMC_1 flexion, 4 = CMC_1 abduction; Fingers: 1 = DIP, 2 = PIP, 3 = MCP)

j: digit (1: thumb, 2: index finger, 3: middle finger, 4: ring finger, 5: little finger)

k: exotendon (1: FET_1, 2: FET_2, 3: FET_3, 4: TET_1, 5: TET_2, 6: TET_3, 7: TET_4)

Approximating a linear relationship between the force and joint angle:

$$\theta_{ij}=\frac{dg_{ij}^k(f_k)}{df_k}f_k+\theta_{ij}|_{f_k=0}\approx p_{ij}^k f_k+q_{ij} \quad (2)$$

where the parameter p_{ij}^k denotes the force-to-angle transformation factor, which demonstrates how the force applied to the k^{th} exotendon converts to the displacement of joint angle θ_{ij}, and the parameter q_{ij} denotes the angular offset in the force-to-angle relationship (i.e., joint angle in the neutral posture).

Given the dataset obtained in Session 1, the transformation parameters for the three FET's were calculated using a linear least-squares estimation.

$$\begin{Bmatrix} p_{ij}^1 \\ p_{ij}^2 \\ p_{ij}^3 \\ q_{ij} \end{Bmatrix} = \left[\begin{Bmatrix} f_1(0) & 0 & 0 & 1 \\ \vdots & \vdots & \vdots & \vdots \\ f_1(3) & 0 & 0 & 1 \end{Bmatrix} \begin{Bmatrix} 0 & f_2(0) & 0 & 1 \\ \vdots & \vdots & \vdots & \vdots \\ 0 & f_2(3) & 0 & 1 \end{Bmatrix} \begin{Bmatrix} 0 & 0 & f_3(0) & 1 \\ \vdots & \vdots & \vdots & \vdots \\ 0 & 0 & f_3(3) & 1 \end{Bmatrix} \right]^p \begin{Bmatrix} \theta_{ij}[f_1(0)] \\ \vdots \\ \theta_{ij}[f_1(3)] \\ \theta_{ij}[f_2(0)] \\ \vdots \\ \theta_{ij}[f_2(3)] \\ \theta_{ij}[f_3(0)] \\ \vdots \\ \theta_{ij}[f_3(3)] \end{Bmatrix} \quad (3)$$

$\mathbf{A}^P$: Pseudo-inverse of the matrix $\mathbf{A}$(i. $\mathbf{A}^P = (\mathbf{A}^T \mathbf{A})^{-1} \mathbf{A}^T$)

$f_k(m)$: Force at level m applied to the k^{th} exotendon (m = 0, 1, 2, 3; 0 corresponds to zero force)

$\theta_{ij}[f_k(m)]$: Flexion angle of the i^{th} joint of the j^{th} digit under the exotendon force $f_k(m)$

With the parameter matrix $\mathbf{P}_k$ that defines the force-angle relationship of exotendon k and the neutral angle matrix $\mathbf{Q}$, the joint angle produced by f_k can be estimated:

$$\mathbf{\Theta} = \mathbf{P_k} \cdot \mathbf{f_k} + \mathbf{Q} \quad (4)$$

$\mathbf{\Theta}(i, j) = \theta_{ij}$: Joint angle of the i^{th} joint of the j^{th} digit

$\mathbf{P}_k(i, j) = p_{ij}^k$: Transformation factor of force at the k^{th} exotendon to joint angle θ_{ij}

$\mathbf{Q}(i, j) = q_{ij}$: Angular offset of joint angle θ_{ij} (i.e., joint angle in neutral posture)

A similar method was used to determine the parameters of the four TETs.

For each exotendon, a repeated measures analysis of variance (ANOVA) was performed to identify potential difference in the transformation parameter p_{ij}^k between joints (i) and digits (j) (within-subject variables), as well as the difference between subject groups (i.e., stroke vs. control and male vs. female; between-subject variables) (IBM SPSS Statistics version 20; IBM Corp., Armonk, NY, USA).

2) Session 2 - Quantification of the kinematic finger workspace—Trajectories of the index fingertip during voluntary movements and during BiomHED actuation were employed to compute the area of the workspace accessed under each condition. Recorded marker coordinates were transformed to a local coordinate system located on the MCP joint of each finger such that the fingertips were always located within a sagittal plane of the phalanges. In these local coordinate systems, the z-axis was aligned with the axis of rotation that characterizes the extension and flexion of the MCP, PIP, and DIP joints, the y-axis with the second metacarpal bone, and the x-axis was defined perpendicular to the palm at the MCP joint. This coordinate system is identical to the system used in a previous study [18].

Two different measures were estimated from the measured finger movements, the kinematic workspace of the fingertip and between-joint coordination patterns within the finger.

a) Kinematic workspace of the index fingertip—Two different kinematic workspace areas were obtained, the workspace reached during voluntary movements and the workspace reached during movements produced by the device. The total workspace was digitized into 900 separate grids (grid size = 0.5 cm × 0.5 cm = 0.25 cm^2). Then, given the trajectory of the index fingertip obtained in each trial, the grids that the fingertip passed through were identified and the workspace areas in the two conditions (voluntary vs. device-assisted) were estimated by multiplying the number of the identified grids by the grid size.

b) Between-joint coordination (PIP–MCP)—During functional hand movements, the spatiotemporal coordination of the PIP and MCP joints was more variable than that of DIP-PIP joints [47–49]. Such increased variability in the PIP–MCP coordination indicates that the PIP and MCP joints need to be controlled independently in order to enable various kinematic patterns of the finger [19,50]. However, this type of independent joint control appears to degrade significantly post-stroke. For instance, in stroke survivors, the use of the PIP and MCP joints during manual task performance was different from that of unimpaired subjects [37].

Therefore, for both voluntary finger movements and the movements produced by the BiomHED, the between-joint coordination of the PIP and MCP joints was examined by estimating 1) the covariance ratio of the PIP and MCP joint movements (R_{PM}), represented by the slope of the linear regression between the joint angles of the PIP and MCP joints (Eq. 5) and 2) the correlation coefficient (r) of the PIP and MCP joint angles during each movement.

$$R_{PM}=\frac{Cov\left[\theta_{PIP},\theta_{MCP}\right]}{Var\left[\theta_{PIP}\right]} \quad (5)$$

$$r=\frac{Cov\left[\theta_{PIP},\theta_{MCP}\right]}{\sqrt{Var\left[\theta_{PIP}\right]}\sqrt{Var\left[\theta_{MCP}\right]}} \quad (6)$$

where

$$Cov\left[X,Y\right]=\frac{1}{N}\sum_{k=1}^{N}X\left(k\right)Y\left(k\right)-\frac{1}{N^2}\sum_{k=1}^{N}X\left(k\right)\sum_{k=1}^{N}Y\left(k\right) \quad \text{and} \quad Var\left[X\right]=\frac{1}{N}\sum_{k=1}^{N}X(k)^2-\left[\frac{1}{N}\sum_{k=1}^{N}X\left(k\right)\right]^2$$

In addition, angle-angle plots of the DIP and PIP joint flexion angles were used to visually depict joint co-variation patterns (PIP-MCP) during these movements.

3) Session 3 - Functional task performance—To determine the exotendon force levels applied to perform the tip-pinch task, the joint angles of the index finger and the thumb of control subjects in the terminal grip posture (during voluntary task performance)

were first estimated and averaged across subjects, providing target joint angles for the tip-pinch task. Then, for each subject, the transformation factor (p_{ij}^{k}) of each exotendon estimated in Session 1 and the target posture were employed to estimate the required magnitude of force applied to each exotendon to generate this posture. Given the target joint angles of the thumb and the index finger (7-by-1 vector) and the force-to-angle transformation factors of each subject (7-by-7 matrix), estimated in the Session 1, the magnitude of each exotendon force was computed by the least-squares estimation (i.e., multiplying pseudo-inverse of the transformation matrix to the target joint angle vector).

To evaluate functional task performance, two kinematic measures were examined. Joint angles of the index finger and the thumb in the final posture during the device-assisted movement were compared to those obtained during voluntary performance by estimating the distance between the index fingertip and thumb tip in the terminal posture using tip marker locations.

Additionally, a sensitivity analysis was performed to gauge the contribution of individual joint angles of the index finger and the thumb on the locations of the index fingertip and thumb tip. A forward kinematics method was used to compute the locations of the fingertip and thumb tip given the segment lengths and the joint angles at the terminal posture. Here, each joint angle was incrementally increased or decreased by 1° during which the change in the between-tip distance was estimated.

III. Results

A. Dynamic function of exotendons

Loading of the individual exotendons produced distinct spatial coordination patterns of the finger and thumb joints, as exemplified by the force-to-angle transformation factor values (p_{ij}^{k}; transformation of k^{th} exotendon force to movement of the i^{th} joint in the j^{th} digit) (Figs. 4 and 5). With the exception of TET_3, the p_{ij}^{k} values of all exotendons were significantly different across joint (all p values < 0.015; Table 3), indicating that distinct spatial coordination patterns were achieved from exotendon loading. For all finger exotendons, there was no significant difference in the transformation factors between digits (all p values > 0.05; Table 3), which implies similar movement patterns for all four digits.

For both subject groups, similar spatial coordination patterns of the finger and thumb were produced by each exotendon, as shown by the within-digit ratio of force-to-angle transformation factors (Fig. 4a vs. 4b and Fig. 4c vs. 4d for control subjects and stroke survivors, respectively). Although the magnitude of the force-to-angle transformation factors for stroke survivors was generally smaller than those for control subjects, this difference was not statistically significant (p = 0.149–0.839; Table 3). The within-digit ratios of the estimated force-to-angle transformation factors of the three exotendons (FET_1 – FET_3) were 19:33:48 (FET_1), 33:40:26 (FET_2), and 15:30:55 (FET_3) for control subjects, and 10:23:67 (FET_1), 33:39:28 (FET_2), and 25:20:55 (FET_3) for control subjects. Overall, the ratios of the estimated force-to-angle transformation factors of the finger exotendons were comparable to

the values obtained from muscle stimulation/tendon excursion experiments reported in the literature (Table 4).

Gender was not a significant factor for any of the FETs and for three of the TETs (TET_1, TET_2, and TET_3). There was a significant gender-effect on TET_4 ($p = 0.022$), such that the p_{41}^7 value from male subjects (mean ± SD = 0.69 ± 0.39 °/N) was significantly smaller than that from female subjects (mean ± SD = 1.79 ± 0.48 °/N). Here, a total of 25 out of 728 (3.4% of the total dataset) values were not used due to the loss of markers during motion capture.

B. Kinematic workspace of the finger

1) Fingertip workspace—For three stroke survivors (Subjects 1–3), the fingertip workspace area, computed from the number of grids that the fingertip accessed during movement, increased by 63–1014% with the assistance of the BiomHED system (Table 5). More importantly, the system allowed these subjects to access different regions of the fingertip workspace (i.e., distal region; Fig. 5) compared to the regions accessed during voluntary movements. For one subject with mild impairment (Subject 4, FM UE score = 40/66), the workspace area accessed by the BiomHED system was slightly smaller than that reached during voluntary movements. For control subjects, the workspace area of the BiomHED system (17.83±3.94 cm^2) was generally smaller than that of voluntary movements (30.30±8.65 cm^2).

2) Spatial joint coordination—For the stroke survivors, the spatial co-variation pattern of the PIP and MCP joints did not vary significantly during voluntary finger movements. The PIP:MCP covariance ratio (R_{PM}, the slope of PIP-MCP correlation) remained approximately constant with a small standard deviation throughout voluntary workspace exploration, resulting in a high correlation coefficient (r) between the PIP and MCP joint angles (mean ± SD r-value: 0.74 ± 0.10; Table 6). This result indicates that the movements of these two joints were highly coupled. In contrast, control subjects had low correlation coefficients (r) between the PIP and MCP joints during voluntary movements (mean ± SD r value: 0.37 ± 0.29), indicating independent control of the two joints.

Distinct joint co-variation (R_{PM}) patterns were obtained from the five exotendon loading conditions (LC_1–LC_5; Table 7a and b; Fig. 6), indicating that the device enabled stroke survivors to produce a range of distinct between-joint finger coordination patterns. Various ranges of motion of the PIP and MCP joints were observed across the loading conditions (i.e., widely different locations of the PIPMCP co-variation lines in the PIP_2-MCP_2 workspace; Fig. 6). This is also indicated by the differences in the mid-range angles of the PIP and MCP joint range of motion for each condition (Table 7c).

C. Functional task performance: tip pinch

Use of the BiomHED system improved the kinematic aspects of functional task performance of stroke survivors. With the assistance of the device, the distance between the fingertip and thumb tip in the terminal grip posture decreased by an average 17.9 mm (Table 8). During unassisted movements, stroke survivors typically adopted a compensatory strategy of using

the palmar aspect of the middle phalanx of the index finger and the dorsal aspect of the thumb tip to hold the object (or vice versa) (Fig. 7a), while the thumb tip was positioned to properly oppose the fingertip base during device-assisted movements (Fig. 7b).

Specifically, the device increased the abduction angle of the thumb CMC joint by an average of 5.3°, which, based on a *post hoc* kinematic analysis, appeared to primarily contribute to a reduction in the between-tip distance. When segment lengths of the subjects were considered, *post hoc* forward kinematics analysis showed that an average 5.3° increase in the CMC abduction angle contributes to an approximate 12–14 mm decrease in the between-tip distance, depending on segment lengths.

IV. Discussion

This study presents a novel robotic device that enables functional task-oriented training of the impaired hands of stroke survivors. The efficacy of this biomimetic design approach (i.e., seven exotendons employed to control 22 DOFs of the hand) to simplify device control while retaining the level of complexity of the task reproduced by the device was tested.

A. Exotendon function: spatial coordination of multi-joint finger movements

The dynamic function of the exotendons, represented by the spatial joint coordination patterns of the movements resulting from loading each exotendon, were comparable to those of the hand muscle-tendon units reported in the literature [33,39,40,42]. However, it should be acknowledged that there is a discrepancy in the literature regarding dynamic function of the FDP [39,40,42]. A previous study [40] showed that the dynamic function of a multi-articular muscle such as the FDP is affected by a number of mechanical factors including passive joint impedance, which in part explains the difference in the coordination patterns between dynamic [40] and static [42]/kinematic [39] measurements. Not surprisingly, the spatial coordination pattern obtained from our exotendon device (FET_2) was similar to the joint coordination pattern of the finger movements resulting from *in vivo* muscle stimulation [40].

Although similar joint coordination patterns were observed for both subject groups in this study, the magnitude of the transformation factors for exotendon force to joint movements (p_{ij}^{k}) was smaller for stroke subjects (Fig. 4). It has been reported that, following stroke, passive joint impedance increases due to both mechanical [51,52] and neurologic [53,54] factors. Therefore, it is likely that an increase in the joint impedance of stroke survivors led to the smaller/lower force-to-angle transformation factors when using the device, although this difference did not reach statistical significance. Passive movements of the hand produced by the exotendon loading may have also induced involuntary activation of some hand muscles, particularly for spastic flexor muscles of stroke survivors, which could have affected the force-to-angle conversion factor estimation. In addition, it should be acknowledged that there was a gender effect on the transformation factor of TET_4 force to the CMC_1 abduction angle (p_{41}^{7}). This effect is likely due to the gender difference in the passive stiffness of the CMC joint $_1$. For instance, it has been reported that females demonstrate more CMC_1 joint laxity than males [54]. Overall, evaluation of exotendon

function demonstrates that the BiomHED is capable of producing functional hand movements in stroke survivors, as the spatial joint coordination patterns produced by the exotendons were similar to those previously reported for human muscle-tendon units [33,39,40,42].

B. Restoration of finger workspace: endpoint area and between-joint coordination

The ability to place/locate the fingertip in a desired location is essential in performing manual tasks. Functional hand tasks require different strategies in order to place the fingers/thumb on specific points/locations on an object depending on the task parameters/constraints, such as task goal [56,57] and geometry of the object [58-60]. As shown in the fingertip workspace (Table 5 and Fig. 5), the BiomHED system allows the fingertip to access a large portion of the possible workspace. However, to demonstrate the capacity of the device to reach different regions of the workspace, only five exotendon loading conditions ($LC_1 - LC_5$) were tested. It is expected that a larger portion of the workspace could be accessed/reached by implementing more exotendon loading conditions.

Importantly, not only did the device restore the range of motion at the endpoint (i.e., the fingertip) but also restored the variability in the between-joint coordination patterns (i.e., PIP–MCP). Correlation between the MCP and PIP joints was generally low during functional hand movements of healthy subjects [48], indicating that these two joints should be controlled independently in order to perform functional tasks. Indeed, in this experiment, the MCP–PIP correlation was low (mean ± SD $r = 0.37 \pm 0.29$) for the control subjects during voluntary workspace exploration. In contrast, MCP–PIP correlation for the stroke survivors was higher (mean ± SD $r = 0.74 \pm 0.10$), suggesting that their ability to independently control these two joints was greatly impaired. An impaired ability to independently control the MCP and PIP joints not only leads to the loss of voluntary workspace of the fingertip, but can also limit the ability to produce a specific contact angle between the fingertip and the object, which may be important in grasping objects of various shapes [61].

C. Functional task performance

When performing manual tasks, many stroke survivors employ (subject-specific) compensatory strategies due to their motor deficit(s) [37]. While some studies have suggested that functional improvement of the hand post-stroke can be mediated through promoting compensatory strategies [62], it is generally thought that promoting the use of proper mechanics during task-oriented training of stroke survivors is ideal for promoting effective functional recovery [35,63,64].

Kinematic measures such as individual joint angles recorded during functional movements are often employed to distinguish ‘true recovery’ and ‘compensation’ in stroke survivors [65]. During the tip-pinch task in this experiment, the primary difference in performance between most stroke survivors, who used compensatory strategies, and unimpaired subjects was the point of contact between the index fingertip and thumb tip (Fig. 7a). The BiomHED device enabled subjects to restore proper task kinematics (Fig. 7b), as indicated by the significant reduction in the distance between the index fingertip and thumb tip. *Post hoc*

analysis showed that decreased thumb abduction was the primary contributor to the compensatory strategy that patients employed. From a kinematic point of view, since the CMC joint is the most proximal joint of the thumb, it has the greatest effect on the location of the thumb tip. Note that thumb abduction is one of the most impaired movements in stroke survivors and restoration of thumb abduction represents significant functional improvement in the hand, based on clinical functionality testing (i.e., Chedoke-McMaster Stroke Assessment Measures; [66,67]).

By overcoming ‘subject-specific’ deficits that induce compensatory strategies, similar approaches can be used to restore the performance of other manual tasks in stroke survivors. As the dynamic function of the exotendons is similar to that of hand muscle-tendon units, kinematic deficits in task performance for each individual patient can be used to identify ‘subject-specific’ deficits in his/her muscle-tendon function, which can then be used to design BiomHED assistance patterns tailored to the specific needs of each subject.

D. Limitations

It should be noted that independent control of the four fingers cannot be achieved by the proposed system, thus more sophisticated hand movements that require independent control of the four fingers cannot be reproduced by the current device design. However, since the device can independently control the thumb and index finger, the BiomHED device can be employed to produce various types of pinch grips. Independent control of the PIP and MCP joints of the finger enables subjects to produce various configurations/postures of the finger.

In addition, some of the hand muscle-tendons were not considered in the design of the proposed device. For instance, flexor digitorum superficialis and flexor pollicis brevis muscle-tendons were not modeled in the proposed system; exclusion of these muscles may limit the capacity of the device to accurately reproduce kinematics of certain manual tasks, for which these excluded muscles are mainly involved. For instance, the ‘within-digit’ spatial coordination patterns of voluntary pinch task were slightly different from those of task performed by the device (Table x). While inclusion of these muscles in the device may allow the device to reproduce the kinematics of these manual tasks more accurately, it could also increase the complexity of the device design and its control schemes.

During workspace exploration, a certain portion of the workspace that corresponds to large total finger flexion angles ( ) cannot be reached by the device, partially because the thermoplastic guides ($\theta_{DIP} + \theta_{PIP} + \theta_{MCP} > 210°$) cannot be reached by the device, partially because the thermoplastic guides on the palmar aspect of the fingers limited finger flexion. Joint range of motion may be increased in future devices by using thinner, smaller thermoplastic guides. However, thinner guides result in a smaller moment arm for each exotendon, which will require stronger actuators to produce the same amount of joint torque. This type of system modification was avoided in the current study due to the safety concerns and the potential for system inefficiency. Since most manual tasks do not require finger postures with extremes of flexion, the inability of the device to reach this portion of the workspace has relatively little functional relevance.

Although the encoder in the motor can record the excursion of each cable, which could then be combined to provide information regarding the total flexion angle of the finger or the thumb, individual joint angles cannot be measured unless an external motion capture system is used concurrently. In order to achieve a more robust control scheme, future designs will include the use of additional transducers, such as piezoresistive bend sensors, to provide individual joint flexion data to the controller. Note that interactions between the individual exotendon forces may exist, as shown by *in vitro* experiments that examined dynamics of the musculotendon structure of the human hand [34], and these interactions must be assessed and properly compensated for to allow precise control of hand movement.

E. Implications

The BiomHED system developed in this study is capable of reproducing the distinct between-joint coordination patterns of human muscle-tendon units. Not only were the thumb and the fingers controlled independently, the PIP and MCP joints within an individual digit were also controlled in a manner similar to intrinsic human finger control. Therefore, the joint coordination patterns reproduced by the device can be combined to produce movement patterns used in different functional tasks of the hand. Accordingly, the BiomHED system is expected to aid in delivering a robot-assisted ‘task-oriented’ training of the hand in stroke survivors. While task-oriented training protocols that enforce use of the impaired hand in daily functional activities have proven to be effective in promoting functional hand recovery [68], most existing protocols involving robot-assisted hand training do not allow patients to practice multiple functional tasks. The proposed system addresses two important elements of effective task-oriented training. The prototype BiomHED system allow users to practice multiple functional tasks and, due to the lightweight design (total system weight including the glove and forearm apparatuŝ 1 kg), allows various arm movements to be combined with hand training. This element is important considering most functional upper extremity tasks involve concurrent control of the arm and hand segments [69].

Furthermore, use of the BiomHED system can allow the subject's participation to be maximized during training. For instance, upon identification of subject-specific deficits in muscle function, the dynamic function of the impaired muscle(s) can be reinforced by applying force to only the corresponding exotendon(s), while intact muscles remain unassisted. This ‘assist-as-needed’ technique will promote the voluntary drive of the patients and maximize their participation in the training.

In addition, due to its lightweight design, the BiomHED system could be used as a wearable orthosis that assist in producing functional movements of the hand for stroke survivors.

V. Conclusion

In this paper, the development and evaluation of the biomimetic hand device, BiomHED, was presented. The actuators (i.e., exotendons) of the BiomHED system were capable of reproducing the distinct joint coordination patterns of human muscle-tendon units, indicating that the device can assist stroke survivors in producing a variety of functional hand movements. The potential of the system was demonstrated by the significant increase in the kinematic workspace of the index finger in stroke survivors, as well as the improvement in

the kinematics of functional task performance. The BiomHED system incorporates key components of effective rehabilitation training in that the proposed system will effectively deliver a robot-assisted 'task-oriented' training of the hand to stroke survivors, while subject participation in the training is also maximized by employing an 'assist-as-needed' strategy. A future training study would be warranted in order to demonstrate the efficacy of the proposed system to improve the functionality of stroke survivors.

Acknowledgments

This work was supported in part by the National Institute of Health (NIH) under Grant 1R03HD74870-01A1 (Lee) and by the NIH intramural research program (Park). The authors would like to thank Drs. Peter S. Lum and Diane L. Damiano for their invaluable input to the study.

REFERENCES

1. Wade DT, Hewer RL, Wood VA, Skilbeck CE, Ismail HM. The hemiplegic arm after stroke: measurement and recovery. J. Neurol. Neurosurgi. Psychiatry. 1983; 46:521–524.
2. Kwakkel G, Wagenaar RC, Kollen BJ, Lankhorst GJ. Predicting disability in stroke: a critical review of the literature. Age Ageing. 1996; 25:479–489. [PubMed: 9003886]
3. Nakayama H, Jorgensen HS, Raaschou HO, Olson TS. Recovery of upper extremity function in stroke patients: the Copenhagen stroke study. Arch. Phys. Med. Rehabil. 1994; 75:394–398. [PubMed: 8172497]
4. Colebatch JG, Gandevia SC. The distribution of muscular weakness in upper motor neuron lesions affecting the arm. Brain. 1989; 112:749–763. [PubMed: 2731028]
5. Mercier C, Bourbonnais D. Relative shoulder flexor and handgrip strength is related to upper limb function after stroke. Clin. Rehabil. 2004; 18:215–221. [PubMed: 15053131]
6. Wing, AM.; Haggard, P.; Flanagan, JR. Hand and Brain: Neurophysiology and Psychology of Hand Movement. Academic Press; New York: 1998.
7. Wilson, FR. The Hand: How its Use Shapes the Brain, Language, and Human Culture. Pantheon; New York: 1999.
8. van Peppen, G. Kwakkel. R.; Wagenaar, RC.; Dauphinee, SW., et al. Effects of augmented exercise therapy time after stroke; a meta-analysis. Stroke. 2004; 35:2529–2539. [PubMed: 15472114]
9. Ringleb PA, Bousser MG, Ford G, Bath P, et al. Guidelines for management of ischaemic stroke and transient ischaemic attack. Cerebrovasc. Dis. 2008; 25:457–507. [PubMed: 18477843]
10. Santello M, Flanders M, Soechting JF. Postural hand synergies for tool use. J. Neurosci. 1998; 18:10105–10115. [PubMed: 9822764]
11. Forssberg H, Eliasson AC, Kinoshita H, Johansson RS, Westling G. Development of human precision grip I: Basic coordination of force. Exp. Brain Res. 1991; 85:451–457. [PubMed: 1893993]
12. Flanagan JR, Wing AM. Modulation of grip force with load force during point-to-point arm movements. Exp. Brain Res. 1993; 95:131–143. [PubMed: 8405245]
13. Kamper DG, Fischer HC HC, Cruz EG EG, Rymer WZ. Weakness is the primary contributor to finger impairment in chronic stroke. Arch. Phys. Med. Rehabil. 2006; 87:1262–1269. [PubMed: 16935065]
14. Trombly, CA. Stroke.. In: Trombly, CA., editor. Occupational therapy for physical dysfunction. Williams & Wilkins; Baltimore: 1989. p. 454-471.
15. Triandafilou KM, Fischer HC, Towles JD, Kamper DG, Rymer WZ. Diminished capacity to modulate motor activation patterns according to task contributes to thumb deficits following stroke. J. Neurophysiol. 2011; 106:1644–1651. [PubMed: 21753022]
16. Lee SW, Triandafilou KM, Lock BA, Kamper DG. Impairment in Task-Specific Modulation of Muscle Coordination Correlates with the Severity of Hand Impairment following Stroke. PLoS ONE. 2013; 8:e68745. [PubMed: 23874745]

17. Miller LC, Dewald JPA. Involuntary paretic wrist/finger flexion forces and EMG increase with shoulder abduction load in individuals with chronic stroke. Clin. Neurophysiol. 2012; 123:1216–1225. [PubMed: 22364723]
18. Cruz EG, Waldinger HC, Kamper DG. Kinetic and kinematic workspaces of the index finger following stroke. Brain. 2005; 128:1112–1121. [PubMed: 15743873]
19. Carpinella I, Jonsdottir J, Ferrarin M. Multi-finger coordination in healthy subjects and stroke patients: a mathematical modelling approach. J. Neuroeng. Rehabil. 2011; 8:19. [PubMed: 21507238]
20. Seo NJ, Rymer WZ, Kamper DG. Altered digit force direction during pinch grip following stroke. Exp. Brain Res. 2010; 202:891–901. [PubMed: 20186401]
21. Fischer HC, Stubblefield K, Kline T, Luo X, Kenyon RV, Kamper DG. Hand rehabilitation following stroke: a pilot study of assisted finger extension training in a virtual environment. Top. Stroke Rehabil. 2007; 14:1–12. [PubMed: 17311785]
22. Jack D, Boian R, Merians AS, Tremaine M, Burdea GC, Adamovich SV, Recce M, Poizner H. Virtual reality-enhanced stroke rehabilitation. IEEE Trans. Neural Syst. Rehabil. Eng. 2001; 9:308–318. [PubMed: 11561668]
23. Takahashi CD, Der-Yeghiaian L, Le V, Motiwala RR, Cramer SC. Robot-based hand motor therapy after stroke. Brain. 2008; 131:425–437. [PubMed: 18156154]
24. Schabowsky CN, Godfrey SB, Holley RJ, Lum PS. Development and pilot testing of HEXORR: Hand EXOskeleton Rehabilitation Robot. NeuroEng. Rehabil. 2010; 7:36.
25. Jones CL, Wang F, Morrison R, Sarkar N, Kamper DG. Design and development of the cable actuated finger exoskeleton for hand rehabilitation following stroke. IEEE ASME Trans. Mechatron. in press.
26. Nef T, Mihelj M, Riener R. ARMin: a robot for patient-cooperative arm therapy. Med. Bio. Eng. Comput. 2007; 45:887–900. [PubMed: 17674069]
27. Park HS, Ren Y, Zhang LQ. IntelliArm: An exoskeleton for diagnosis and treatment of patients with neurological impairments. 2nd IEEE RAS & EMBS Int. Conf. Biomed. Robot Biomechatron. 2008:109–114.
28. Wolbrecht ET, Chan V, Reinkensmeyer DJ. Optimizing compliant, model-based robotic assistance to promote neurorehabilitation. IEEE Trans. Neural Syst. Rehabil. Eng. 2008; 16:286–297. [PubMed: 18586608]
29. Maier MA, Hepp-Reymond MC. EMG activation patterns during force production in precision grip. I. Contribution of 15 finger muscles to isometric force. Exp. Brain Res. 1995; 103:108–122. [PubMed: 7615027]
30. Valero-Cuevas FJ. Predictive modulation of muscle coordination pattern magnitude scales fingertip force magnitude over the voluntary range. J. Neurophysiol. 2000; 83:1469–1479. [PubMed: 10712473]
31. Kutch JJ, Kuo AD, Bloch AM, Rymer WZ. Endpoint force fluctuations reveal flexible rather than synergistic patterns of muscle cooperation. J. Neurophyiol. 2008; 100:2455–2471.
32. Valero-Cuevas FJ, Zajac FE, Burgar CG. Large index-fingertip forces are produced by subject-independent patterns of muscle excitation. J. Biomech. 1998; 31:693–703. [PubMed: 9796669]
33. Lee SW, Chen H, Towles JD, Kamper DG. Estimation of the effective static moment arms of the tendons in the index finger extensor mechanism. J. Biomech. 2008; 41:1567–1573. [PubMed: 18387615]
34. Valero-Cuevas FJ, Yi JW, Brown D, McNamara RV, Paul C, Lipson H. The tendon network of the fingers performs anatomical computation at a macroscopic scale. IEEE Trans. Biomed. Eng. 2007; 54:1161–1166. [PubMed: 17549909]
35. Krakauer JW. Motor learning: its relevance to stroke recovery and neurorehabilitation. Curr. Opi. Neurol. 2006; 19:84–90.
36. Roby-Brami A, Feydy A, Combeaud M, et al. Motor compensation and recovery for reaching in stroke patients. Acta. Neurol. Scand. 2003; 107:369–281. [PubMed: 12713530]
37. Raghavan P, Santello M, Gordon AM, Krakauer JW. Compensatory motor control after stroke: an alternative joint strategy for object-dependent shaping of hand posture. J. Neurophysiol. 2010; 103:3034–3043. [PubMed: 20457866]

38. Garcia-Elias M M, An KN, Berglund L, Linscheid RL, Cooney WP, Chao EYS. Extensor mechanism of the fingers. I. A quantitative geometric study. J. Hand Surg. 1991; 16:1130–1136.
39. An KN, Ueba Y, Chao EY, Cooney WP, Linscheid RL. Tendon excursion and moment arm of index finger muscles. J. Biomech. 1983; 16:419–425. [PubMed: 6619158]
40. Lee SW, Kamper DG. Modeling of multiarticular muscles: Importance of inclusion of tendon-pulley interactions in the finger. IEEE Trans. Biomed. Eng. 2009; 56:2253–2262. [PubMed: 19362899]
41. Valero-Cuevas FJ, Johanson ME, Towles JD. Towards a realistic biomechanical model of the thumb: the choice of kinematic description may be more critical than the solution method or the variability/ uncertainty of musculoskeletal parameters. J. Biomech. 2003; 36:1019–1030. [PubMed: 12757811]
42. Kamper DG, Waldinger HC, Cruz EG. Impact of finger posture on mapping from muscle activation to joint torque. Clin. Biomech. 2006; 21:361–369.
43. Napier JRJR. The prehensile movements of the human hand. J. Bone Joint Surg. 1956; 38B:902–913.
44. Elliott JM, Connolly KJ. A classification of manipulative hand movements. Dev. Med. Child Neurol. 1984; 26:283–296. [PubMed: 6734945]
45. Blennerhassett JM, Carey LM, Matyas TA. Clinical measures of handgrip limitation relate to impaired pinch grip force control after stroke. J. Hand Ther. 2008; 21:245–252. [PubMed: 18652969]
46. Nowak DA. The impact of stroke on the performance of grasping: Usefulness of kinetic and kinematic motion analysis. Neurosci. Biobehav. Rev. 2008; 32:1439–1450. [PubMed: 18582943]
47. Cole KJ, Abbs JH. Coordination of three-joint digit movements for rapid finger-thumb grasp. J. Neurophysiol. 1986; 55:1407–1423. [PubMed: 3734863]
48. Kamper DG, Cruz EG, Siegel MP. Stereotypical fingertip trajectories during grasp. J. Neurophysiol. 2003; 90:3702–3710. [PubMed: 12954607]
49. Kuo PL, Lee DL, Jindrich DL, Dennerlein JT. Finger joint coordination during tapping. J. Biomech. 2006; 39:2934–2942. [PubMed: 16376353]
50. Sangole AP, Levin MF. A new perspective in the understanding of hand dysfunction following neurological injury. Top. Stroke Rehabil. 2007; 14:80–94. [PubMed: 17573314]
51. Dietz V, Trippel M, Berger W. Reflex activity and muscle tone during elbow movements in patients with spastic paresis. Ann. Neurol. 1991; 30:767–769. [PubMed: 1789693]
52. O'Dwyer NJ, Ada L, Neilson PD. Spasticity and muscle contracture following stroke. Brain. 1996; 119:1737–1749. [PubMed: 8931594]
53. Given JD, Dewald JPA, Rymer WZ. Joint dependent passive stiffness in paretic and contralateral limbs of spastic patients with hemiparetic stroke. J. Neurol. Neurosurg. Psychiatry. 1995; 59:271–279. [PubMed: 7673955]
54. Kamper DG, Harvey RL, Suresh S, Rymer WZ. Relative contributions of neural mechanisms versus muscle mechanics in promoting finger extension deficits following stroke. Muscle Nerve. 2003; 28:309–318. [PubMed: 12929190]
55. Wolf JM, Scher DL, Etchill EW, Scott F, Williams AE, Delaronde S, King KB. Relationship of relaxin hormone and thumb carpometacarpal joint arthritis. Clin. Orthop. Relat. Res. DOI 10.1007/s11999-013-2960-4, 2013.
56. Cutkosky MR. On grasp choice, grasp models, and the design of hands for manufacturing tasks. IEEE Trans. Robot. Autom. 1989; 5:269–279.
57. Mackenzie, CL.; Iberall, T. The Grasping Hand. Elsevier Science; Amsterdam: 1994.
58. Santello M, Soechting JF. Gradual molding of the hand to object contours. J. Neurophysiol. 1998; 79:1307–1320. [PubMed: 9497412]
59. Schettino LF, Adamovich SV, Poizner H. Effects of object shape and visual feedback on hand configuration during grasping. Exp. Brain Res. 2003; 151:158–166. [PubMed: 12783144]
60. Lee SW, Zhang X. Development and evaluation of an optimization-based model for power-grip posture prediction. J. Biomech. 2005; 38:1591–1597. [PubMed: 15958215]

61. Kleinholdermann U, Brenner E, Franz VH, Smeets JB. Grasping trapezoidal objects. Exp. Brain Res. 2007; 180:415–420. [PubMed: 17310376]
62. Kitago T, Liang J, Huang VS, Hayes S, Simon P, Tenteromano L, Lazar RM, Marshall RS, Mazzoni P, Lennihan L, Krakauer JW. Improvement after constraint-induced movement therapy: Recovery of normal motor control or task-specific compensation? Neurorehabil. Neural Repair. 2013; 27:99–109. [PubMed: 22798152]
63. Michaelsen SM, Dannenbaum R, Levin MF. Task-specific training with trunk restraint on arm recovery in stroke: randomized control trial. Stroke. 2006; 37:186–192. [PubMed: 16339469]
64. Wu C, Chen Y, Chen H, Lin K, Yeh I. Pilot trial of distributed constraint-induced therapy with trunk restraint to improve poststroke reach to grasp and trunk kinematics. Neurorehabil. Neural Repair. 2012; 26:247–255. [PubMed: 21903975]
65. Levin MF, Kleim JA, Wolf SL. What do motor “recovery” and “compensation” mean in patients following stroke? Neurorehabil. Neural Repair. 2009; 23:313–319. [PubMed: 19118128]
66. Gowland C, Stratford P, Ward M, Moreland J, Torresin W, van Hullenaar S, Sanford J, Barreca S, Vanspall B, Plews N. Measuring physical impairment and disability with the Chedoke-McMaster Stroke Assessment. Stroke. 1993; 24:58–63. [PubMed: 8418551]
67. Barreca S, Gowland CK, Stratford P, Huijbregts M, Griffiths J, Torresin W, Dunkley M, Miller P, Masters L. Development of the Chedoke Arm and Hand Activity Inventory: theoretical constructs, item generation, and selection. Top. Stroke Rehabil. 2004; 11:31–42. [PubMed: 15592988]
68. Wolf SL, Winstein CJ, Miller JP, et al. Effect of constraint-induced movement therapy on upper extremity function 3 to 9 months after stroke. JAMA. 2006; 296:2095–2104. [PubMed: 17077374]
69. Flanagan JR, Tresilian JR. Grip force coupling: a general control strategy for transporting objects. J. Exp. Psychol. Hum. Percept. Perform. 1994; 20:944–957. [PubMed: 7964530]

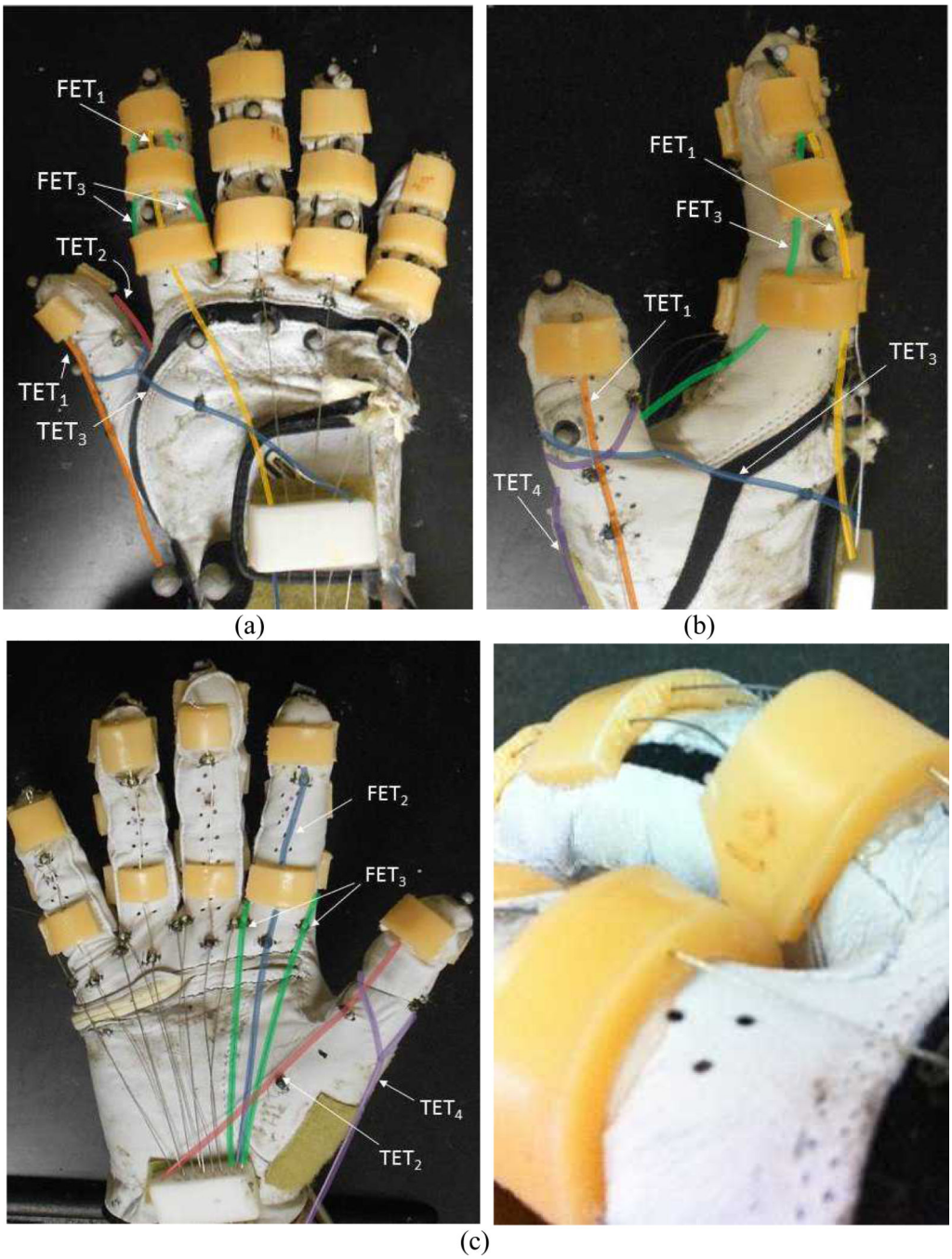

Fig. 1.

Exotendon configuration of the Biomimetic Hand Exotendon Device (BiomHED): (a) dorsal view, (b) radial view, (c) palmar view, and (d) magnified view of the dorsal thermoplastic guides that route exotendons (FET_1 and FET_3). Different colors were used to describe exotendon paths (FET_1: yellow, FET_2: blue, FET_3: green, TET_1: orange, TET_2: pink, TET_3: dark blue, TET_4: magenta).

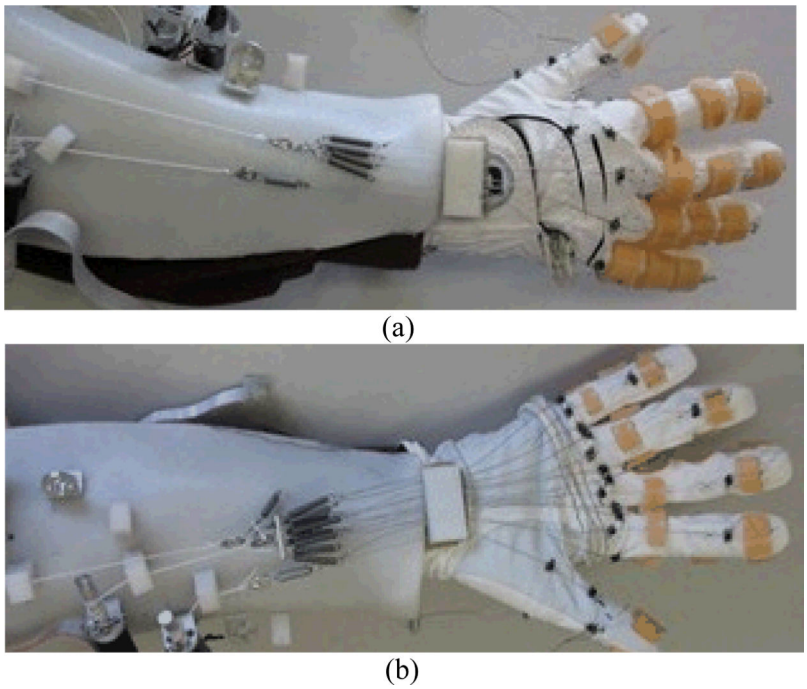

Fig. 2.
The BiomHED system worn by a user: (a) dorsal side, (b) ventral side.

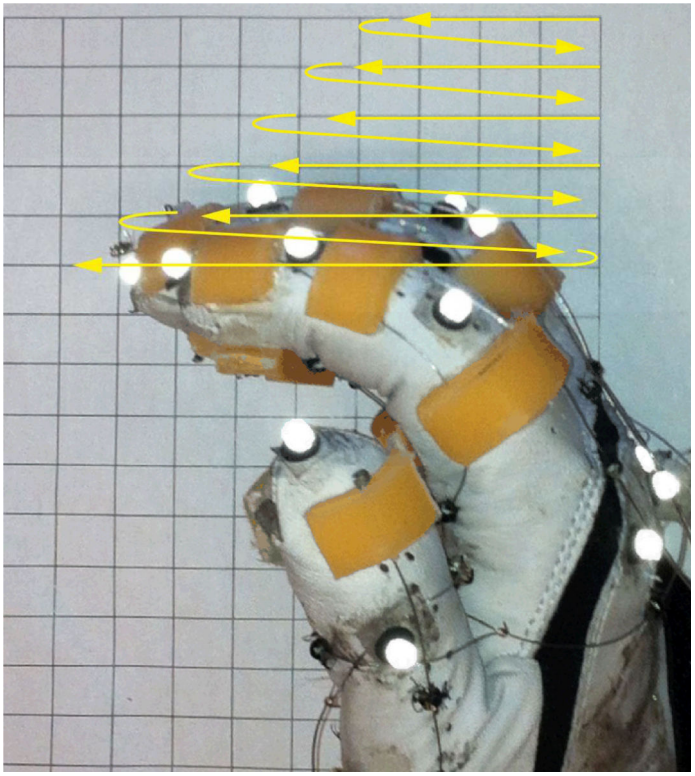

Fig. 3.
Exploration of voluntary finger workspace. The yellow lines indicate the trajectory of the index fingertip.

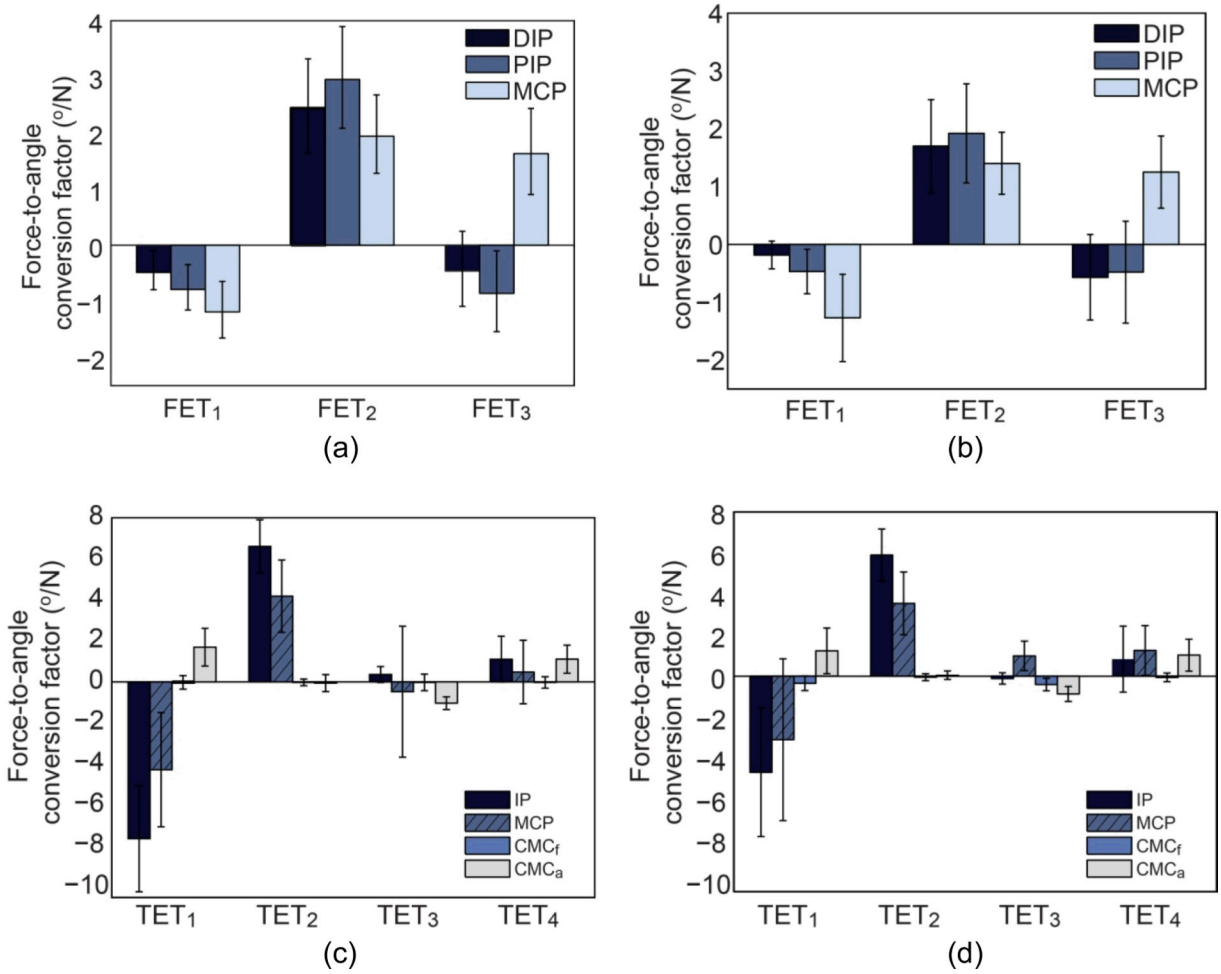

Fig. 4.

Mean (SD) of the force-angle transformation factor (p_{ij}^k) of the three finger exotendons for (a) control subjects and (b) stroke survivors, and mean (SD) of the p_{ij}^k of the thumb exotendons for (c) control subjects and (d) stroke survivors.

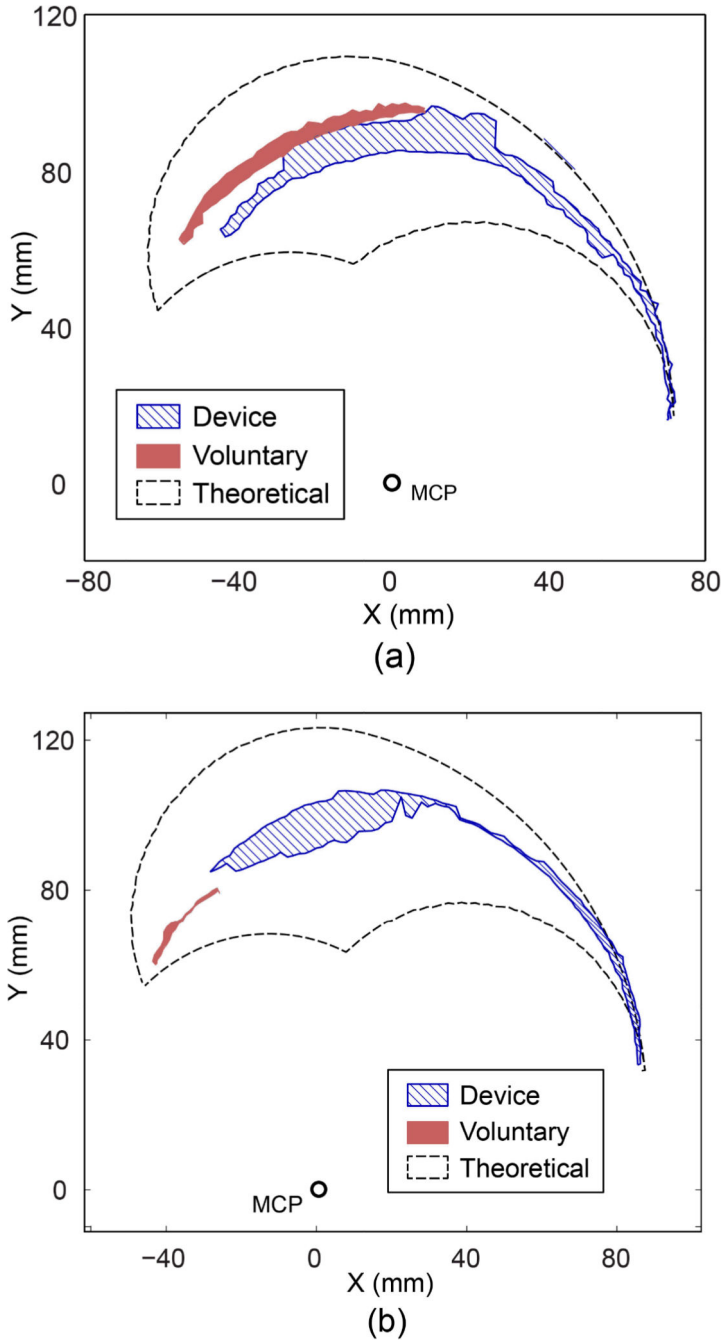

Fig. 5.

Finger workspace accessed during voluntary and device-assisted movements of (a) Subject 2 (UE FM score = 33/66; 146% increase) and (b) Subject 3 (UE FM score = 10/66; 1014% increase).

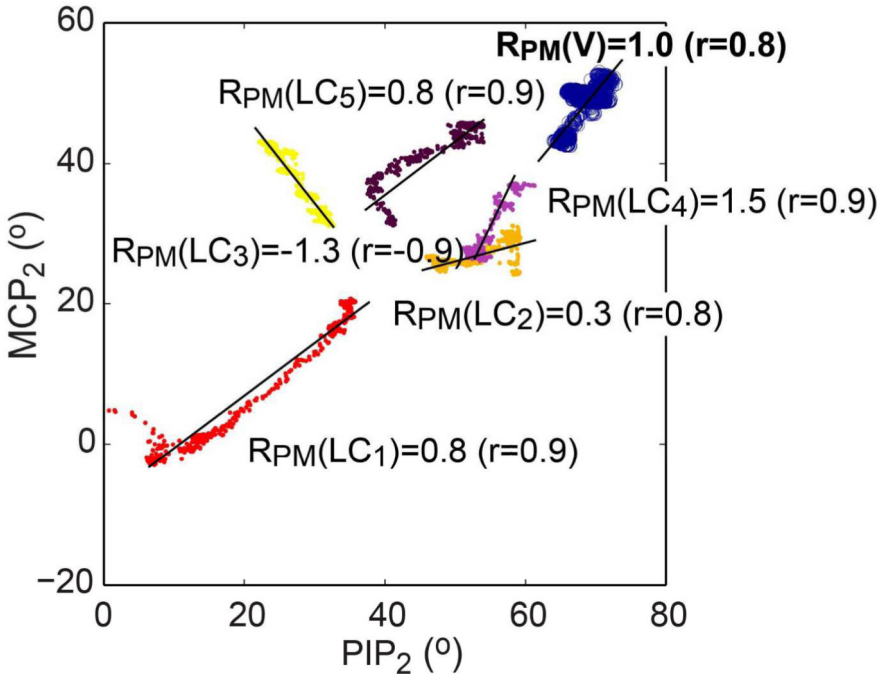

Fig. 6.

Representative angle-angle plot (PIP_2-MCP_2) showing PIP_2–MCP_2 ratios obtained during voluntary movements, $R_{PM}(V)$ (circle) and five movements under five exotendon loading conditions, $R_{PM}(LC_1)$–$R_{PM}(LC_5)$ (dots) for Subject 3 (Trial 1). Not only did the PIP–MCP ratio vary substantially across five exotendon LCs, but the ranges of motion for the two joints also varied substantially under these conditions, as indicated by the differences in the mid-range angles of the range of motion. Note that a very limited region of this workspace was accessed during voluntary movement.

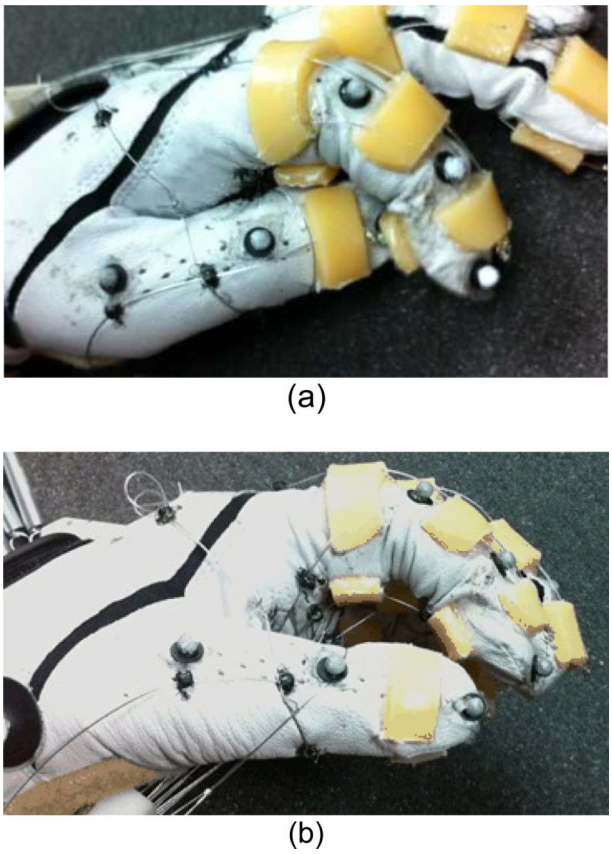

Fig. 7.

Tip pinch task performed by a stroke survivor (Subject 1): (a) Voluntary task performance, (b) device-assisted task performance. Without assistance (a), the subject used a compensatory strategy in that an object was held in position between the dorsal aspect of the distal phalanx of the thumb and the palmar aspect of the distal phalanx of the index finger.

Table 1

Mean (SD) of the geometric moment arm (mm) of the seven exotendons obtained from exotendon excursion-joint rotation data (n = 5): (a) FETs; (b) TETs. Negative denotes joint extension or adduction.

(a) FETs

Joint	Exotendon		
	FET_1	**FET_2**	**$FET_{3/4}$**
DIP_2	−5.4 (0.5)	6.0 (1.2)	−3.4 (0.8)
PIP_2	−6.1 (0.4)	14.3 (1.1)	−0.8 (0.6)
MCP_2	−9.4 (1.1)	21.0 (1.6)	16.9 (7.2)

(b) TETs

Joint	Exotendon			
	TET_1	**TET_2**	**TET_3**	**TET_4**
IPi	8.3 (1.5)	9.7 (1.3)	-	-
MCP_1	14.7 (4.2)	14.4 (2.1)	-	-
CMCi	-	-	−38.0 (5.1)	12.0 (4.1)

Table 2

Subject characteristics of stroke survivors

Subject Number	Gender	Age	Years since Stroke	Dominant Hand	Affected Hand	Upper Extremity Fugl-Meyer Score
1	Male	35	4	Right	Left	16/66
2	Male	65	3	Right	Right	33/66
3	Male	66	N/A	Right	Right	10/66
4	Female	36	5	Right	Right	40/66

Table 3

p-values of the between- and within-subject factors for each of the seven exotendons from a repeated-measures ANOVA

Exotendon	Joint	Digit	Gender	Group
FET_1	0.000	0.307	0.780	0.648
FET_2	0.014	0.074	0.625	0.149
FET_3	0.000	0.154	0.475	0.534
TET_1	0.000	N/A	0.226	0.839
TET_2	0.000		0.061	0.823
TET_3	0.145		0.356	0.271
TET_4	0.015		0.022	0.511

Table 4

Ratio of the three finger joint moments/movements obtained from muscle stimulation or tendon excursion, reported in previous *in vivo* and *in vitro* studies (negative denotes joint extension).

Finger muscle-tendon	Reference	Ratio (DIP:PIP:MCP)*
EDC	An *et al*, 1983[1)]	−13 : −24 : −61
	Kamper *et al*, 2006[2)]	−13 : −23 : −63
	Lee *et al*, 2008[3)]	−18 : −25 : −57
FDP	An *et al*, 1983	18 : 35 : 47
	Kamper *et al.*, 2006	13 : 33 : 54
	Lee and Kamper, 2009[4)]	24 : 51 : 25
INT**	An *et al*, 1983	−14 : −24 : 61
	Kamper *et al.*, 2006	−24 : −11 : 65
	Lee *et al*, 2008	−16 : −3 : 81

* Each ratio vector is normalized to the sum of its absolute value (%). Negative: joint extension; Positive: joint flexion.

** INT (intrinsic muscle) indicates measurement from either first palmar interosseous or lumbricalis muscles. 1)Joint rotation - tendon excursion relationship measured from cadaveric specimens (kinematic; dynamic) 2)Joint moment estimated from *in vivo* electrical stimulation of muscle (kinetic; static) 3)Joint moment estimated from individual tendon loading on cadaveric specimens (kinetic; static) 4)Joint rotation estimated from *in vivo* electrical stimulation of the muscle (kinetic; dynamic)

Table 5

Finger workspace area accessed during (a) voluntary movements and (b) device-assisted movements of stroke survivors. The percent increase in the area from (a) to (b) is shown in (c).

	Finger workspace		
Subject Number	**(a) Voluntary (cm^2)**	**(b) BiomHED (cm^2)**	**(c) Increase (%)**
1	8.00	13.00	63
2	7.00	17.25	146
3	1.75	19.50	1014
4	18.50	14.75	−20

Table 6

Spatial coordination of PIP-MCP joints of stroke survivors during voluntary movements. Mean ± SD of (a) PIP:MCP ratio (R_{PM}) and (b) correlation coefficient (r)

	Subject number				Mean (SD)
	1	2	3	4	
(a) R_{pm}	1.17 (0.15)	0.67 (0.06)	0.73 (0.23)	0.43 (0.06)	0.75 (0.31)
(b) r	0.77 (0.11)	0.87 (0.06)	0.73 (0.11)	0.60 (0.10)	0.74 (0.10)

Table 7

Spatial coordination of PIP_2 and MCP_2 joints under the five exotendon loading conditions (LC_1-LC_5) and during voluntary movements: mean (SD) values of (a) PIP_2:MCP_2 ratio RPM of the stroke and control subjects, (b) correlation coefficient (*r*) of the stroke and control subjects, and (c) mean (SD) of the PIP_2 and MCP_2 joint angles of the stroke subjects.

Movement production		**(a) R_{pm}**		**(b) *r***		**(c) Mid-angle of ROM (°)**	
		Stroke	**Control**	**Stroke**	**Control**	**PIP_2**	**MCP_2**
Exotendon loading conditions (LCs)	LC_1	1.51 (1.10)	1.57 (0.65)	0.63 (0.36)	0.90 (0.08)	24.8 (8.8)	20.5 (7.3)
	LC2	0.92 (0.30)	0.54 (0.18)	0.94 (0.05)	0.92 (0.08)	42.4 (7.3)	35.4 (9.4)
	LC3	−1.43 (0.49)	−1.68 (0.79)	−0.92 (0.15)	−0.88 (0.11)	27.3 (11.7)	36.4 (9.8)
	LC4	1.65 (0.90)	0.66 (0.19)	0.84 (0.09)	0.80 (0.15)	43.7 (8.1)	35.2 (8.7)
	LC5	0.78 (0.24)	0.58 (0.21)	0.72 (0.13)	0.89 (0.06)	43.7 (14.2)	41.7 (7.6)
Voluntary movement (V)		0.75 (0.31)	0.37 (0.27)	0.74(0.10)	0.17 (0.21)	47.6 (14.2)	0.74(0.10)

Table 8

Kinematic measurements from the tip-pinch task (VOL: voluntary movement, DEV: movement produced by the device): (a) mean and standard deviation of the joint angles (°) of the index finger and the thumb in the tip-pinch posture, (b) reduction in distance between tips during device-assisted movement (compared to voluntary movement).

Group	Movement type	(a) Joint angle (°)							(b) Reduction in distance between tips Δd (mm)
		Index finger				Thumb			
		DIP	PIP	MCP	IP	MCP	CMC(f)	CMC(a)	
Stroke (*n* = 4)	VOL	37.0 (7.7)	56.3 (10.4)	37.0 (22.3)	44.3 (17.1)	26.0 (18.3)	31.3 (9.8)	32.5 (3.7)	17.9 (15.3)
	DEV	31.7 (13.7)	48.4 (6.0)	27.1 (12.7)	46.2 (8.5)	19.3 (15.2)	33.2 (5.6)	37.8 (2.8)	
Control (*n* = 10)	VOL	26.0 (10.6)	40.4 (10.2)	23.8 (7.3)	24.6 (17.8)	19.5 (12.0)	39.8 (6.1)	40.4 (6.3)	−0.9 (6.5)
	DEV	31.8 (6.3)	49.7 (6.7)	24.5 (8.0)	47.9 (7.3)	27.9 (9.5)	36.1 (6.5)	39.9 (5.9)	